Journal of Machine Engineering, 2023, Vol. 23
ISSN 1895-7595 (Print) ISSN 2391-8071 (Online)

Received: *24 April 2023* / Accepted: *29 May 2023* / Published online: *08 June 2023*

machine safety, polycarbonate, aging, finite element simulation

Eckart UHLMANN[1,2], Mitchel POLTE[1,2],
Nils BERGSTRÖM[1*], Vu Ninh LE[2]

MODELLING THE AGE-RELATED DECREASE IN BALLISTIC LIMIT VELOCITY OF POLYCARBONATE VISION PANELS USING A JOHNSON-COOK MATERIAL MODEL COUPLED WITH VARIABLE FAILURE CRITERIA

Machine tools are equipped with polycarbonate vision panels that allow the operator to observe the machining process and protect him from ejected fragments. Adequate protection is demonstrated by impact tests. However, polycarbonate is subject to aging processes, which diminish the protective performance of such panels. This paper presents an approach for modelling aging effects on the ballistic limit velocity of polycarbonate using Finite Element simulations. A Johnson-Cook material model in conjunction with variable failure criteria was used for the simulations. Aging effects on the ballistic limit velocity were included in the model by adjusting the failure criteria. Material parameters and failure criteria were derived from experimental impact and tensile tests on unaged and aged polycarbonate specimen. The numerical results predict the ballistic limit velocity with a maximum deviation of 0.98%. The model provides a more in-depth understanding of the aging effects on the safety performance of polycarbonate vision panels.

1. INTRODUCTION

Polymers are increasingly being used for applications that involve exposure to high dynamic loads. Polycarbonate (PC), for instance, is used as material for vision panels in machine tool safeguards. As such, they fulfil two functions: On the one hand, they prevent the operator from accessing hazardous areas and, on the other hand, they hold back ejected workpieces or tool parts in the event of an accident [1]. To ensure a sufficient protection PC-vision panels must comply with international standards, such as ISO 14120 [2], which provides general guidelines for testing the protective performance of safeguards in machine tools. Depending on the machine type, these guidelines are further specified in dedicated standards, such as ISO 23125 [3] for lathes. In any case, the guard is subjected to an impact by a blunt projectile, whereby the shape and the mass of the projectile m_{pr} depend on the

[1] Institute for Machine Tools and Factory Management, TU Berlin, Germany
[2] Fraunhofer Institute for Production Systems and Design Technology IPK, Fraunhofer, Germany
[*] E-mail: bergstroem@iwf.tu-berlin.de
https://doi.org/10.36897/jme/166600

respective machine type. As measures of the protective performance of safeguards, two properties are generally being used:

- the impact resistance (IR) Y and
- the ballistic limit velocity (BLV) v_{bl}.

Traditionally, the IR Y has been the measure of choice in research, since it is the property referred to in international standards [2, 3]. It is defined as maximum kinetic projectile energy E_{pr} a safeguard is able to withstand when subjected to an impact. A test is considered to be passed as long as it results only in elastic-plastic deformations with incipient cracks. As soon as the deformation yields a continuous crack, visible on both sides of the safeguard, the test is considered failed. However, in recent years the BLV v_{bl} is increasingly used when evaluating the performance of safeguards in machine tools under ballistic load. It is defined as initial projectile velocity $v_{pr,i}$ that is required for a projectile to emerge from the safeguard with a residual projectile velocity of $v_{pr,r}$ = 0 m/s [4]. Figure 1 shows characteristic damage patterns of PC-vision panels used to determine the IR Y and BLV v_{bl}. Regardless of the metric used, the protective performance of PC-vision panels is significantly influenced by a number of parameters, such as:

- the width w_{PC}, height h_{PC} and thickness t_{PC} of the PC-vision panel [5],
- the location of the projectile impact [6] and
- aging processes [7, 8].

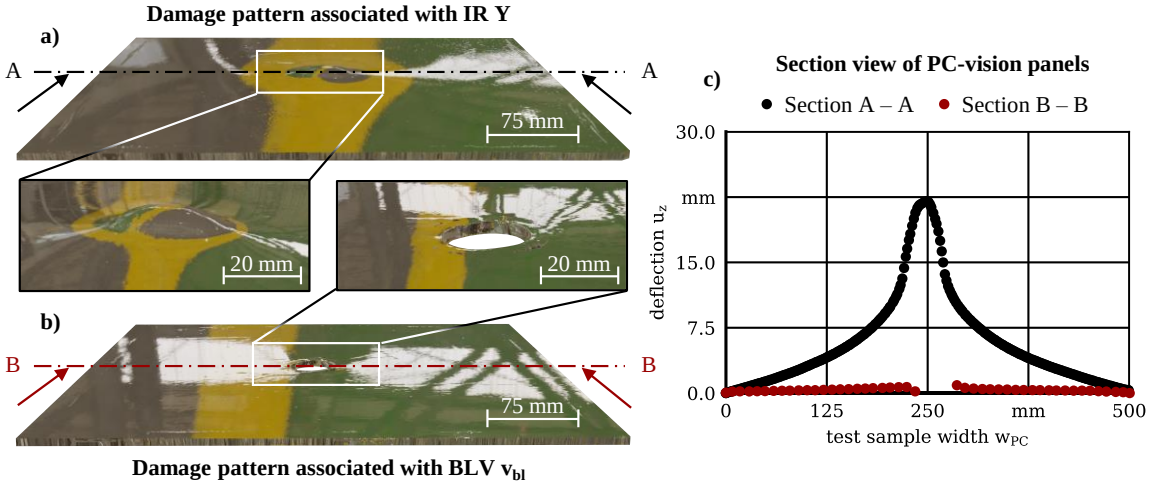

Fig. 1. Characteristic damage patterns of PC-vision panels after impact test; a) PC-vision panel that passed an impact test; b) PC-vision panel that failed an impact test; c) Section view and deflection u_z for both vision panels

Of the above listed parameters, aging processes are the least understood to date. Thus, ensuring a constant safety performance of PC-vision panels over several years operating time t_o is still challenging. As a polymer PC is subject to aging processes that generally cause a deterioration of its mechanical properties and results in a decrease of IR Y or BLV v_{bl}, respectively. The aging of PC is predominantly driven by thermal oxidation, photodegradation and hydrolysis [9]. Thermal oxidation is of minor importance from safety point of view, since it affects mainly its optical properties and results in a yellowing of the PC-vision panel. The effect of photodegradation on the mechanical properties of PC was studied by Landi et al. [10] who exposed PC to ultraviolet (UV) light using a weathering tester.

Subsequently conducted impact tests showed no significant effect on mechanical properties of the PC-vision panels. Hydrolysis-related aging, however, is crucial for the safety performance of PC-vision panels in machine tools. The catalytic effect of alkaline cooling lubricants (CL) leads to a deterioration of its mechanical properties [9]. Duchstein [8] studied the effect of CL on the IR Y of PC by spraying PC-sheets with a CL-emulsion over a period of t_{exp} = 50 weeks. As result of the CL-exposure, a decrease in IR Y by 35% was observed. These results are consistent with prior research by Bold [7] who aged PC-sheets in immersion bath tests and found a similar decrease in impact resistance Y of approximately 40% after an exposure time of t_{exp} = 14 days.

A common characteristic of all the above mentioned studies [6–8, 10] is the substantial material and experimental effort they require. A joint investigation of all parameters, including possible interaction between them, has not been conducted so far, partly due to the considerable experimental effort associated to such a study. Simulations, however, allow a significant reduction in experimental effort. When properly validated they permit the analysis of large sets of parameters and study conditions they were not considered in experiments. Based on this premise, this paper presents an approach to model the CL-related decrease in BLV v_{bl} of PC-vision panels using Finite Element (FE)-simulations. A Johnson-Cook (JC) material model in conjunction with variable failure criteria is used for the simulations. The material model and the failure criteria are based on experimental tensile and impact tests, which were carried out for unaged and aged PC-specimen. Aging of the PC-specimen was accomplished by immersion bath tests in a CL-emulsion for an exposure time of t_{exp} = 8 weeks. The numerical results of the are in good accordance with the experimental findings with a maximum deviation of 0.98% providing an effective method for including aging effects in FE-simulations for future studies to come.

2. EXPERIMENTAL SETUP

Aging tests

For a characterization of the mechanical properties of PC and the CL-induced aging effects on them, a series of aging tests were carried out. For this purpose, PC-specimen were placed in a CL-emulsion composed of 90% water and 10% CL. A reference fluid under the name VSI 034 PE defined by Verband Schmierstoff Industrie e.V. (VSI), Hamburg, Germany was utilized as CL. This alkaline CL has been used in previous studies on CL-related aging of PC in machine tools by Uhlmann et al. [11] and is suspected to be among the CL, which cause the most severe decrease in BLV v_{bl}. Type 1BA tensile specimen according to ISO 527-2 [12], as well as square PC-sheets with a width of w_{PC} = 300 mm and a thickness of t_{PC} = 12 mm were used as specimens. The exposure time t_{exp} was chosen following previous aging tests by Bold [7], who exposed PC-sheets to CL over a period of t_{exp} = 2 weeks. Given that the composition of the CL applied in this study differs from the CL used by Bold [7], the CL-induced aging effect was unknow prior to this investigation. Therefore, a fourfold exposure time of t_{exp} = 8 weeks was adopted to ensure a distinctive and pronounced aging effect could be observed in this study.

Tensile test

Quasi-static tensile tests were performed to investigate the aging-effect on yield stress σ_y and the strain at break ε_b. Since PC is highly dependent on the strain rate $\dot{\varepsilon}$ [13], these tensile tests were carried out for five different test velocities ranging from 10 mm/min $\leq v_t \leq$ 900 mm/min. Each test included a total number of $n_t = 5$ tensile tests and was conducted for both unaged and for aged specimen. A tensile testing machine of type T1-FR150SN.A4K from ZwickRoell GmbH & Co. Kg, Ulm, Germany was used to perform the tensile tests.

Impact tests

In addition to the tensile tests two series of impact tests were conducted, both for aged and unaged PC-sheets with the aim to study the CL-related aging effects on the BLV v_{bl}. The impact tests were carried out at the test facility of the Institute for Machine Tools and Factory Management (IWF) of the TU Berlin, see Fig. 2. The velocity of the projectile $v_{pr,i}$ is controlled by the pressure p in the pressure tank and the acceleration length l_a of the barrel. A light barrier between the barrel muzzle and the PC-sheet is used for measuring the projectile velocity $v_{pr,i}$. The impact test facility is equipped with two high-speed cameras. One was placed in front of the PC-sheet to capture the impact, while the second high-speed camera was placed behind the PC-sheet to measure the residual projectile velocity $v_{pr,r}$, after penetrating the PC-sheet. The PC-sheet is attached to the test sample frame with screw clamps with an overlapping width of w_{ov} = 25 mm. The test sample frame in turn is attached to the test sample mount by screw clamps, as shown in Fig. 2b.

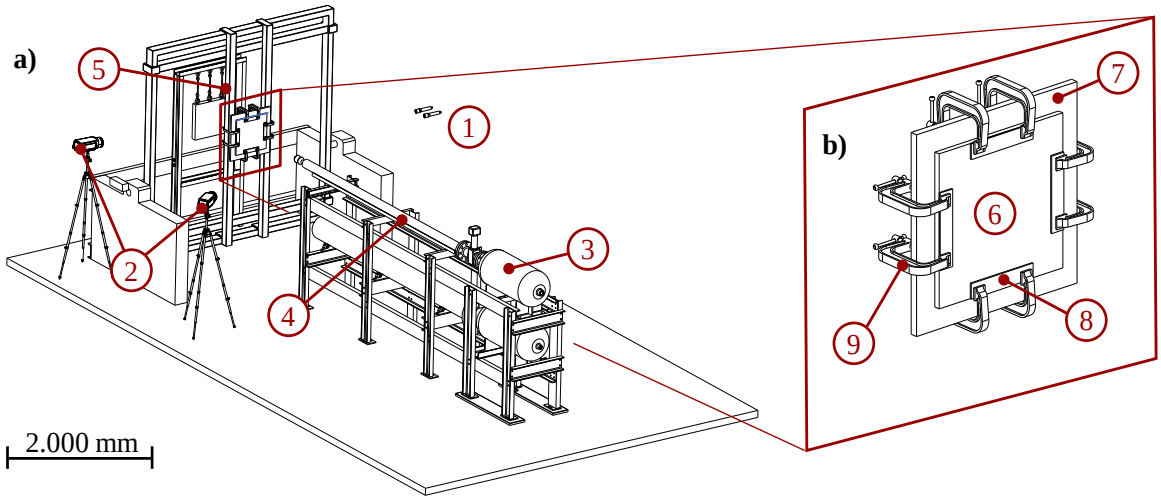

1 Light barrier
2 High-speed camera
3 Pressure tank
4 Barrel
5 Test sample mount
6 PC-sheet
7 Test sample frame
8 Fastening profiles
9 Screw clamps

Fig. 2. Impact test facility; a) Isometric view of entire test facility; b) Detailed view of the mounting conditions of the PC-sheets

The PC-sheets were subjected to a central impact. The impact tests were conducted according to ISO 23125 [3] using a steel projectile of mass m_{pr} = 2.5 kg, as shown in Fig. 3.

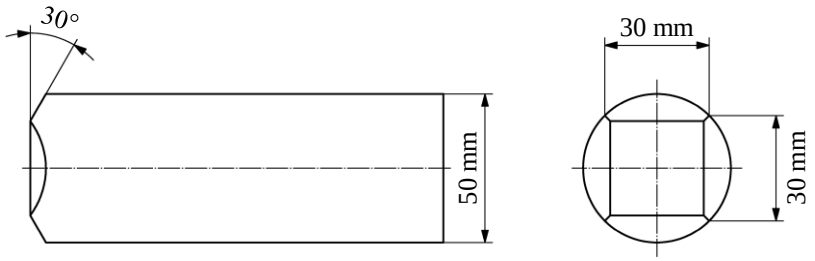

Fig. 3. Standardized projectile of projectile mass m_{pr} =2.5 kg according to ISO 23125 [3]

The BLV v_{bl} is determined according to an analytical model by Recht and Ipson [14]. For a rigid projectile the model describes the residual projectile velocity $v_{pr,r}$ as a function of the initial projectile velocity $v_{pr,i}$ and the BLV v_{bl} [15], as shown in Eq. (1).

$$v_{pr,r} = a \cdot \left(v_{pr,i}^2 - v_{bl}^2\right)^{1/2} \tag{1}$$

Both, the unknown parameter a as well as the BLV v_{bl} are calculated by means of a least square approximation. Figure 4 provides an exemplary illustration of an impact test series and the approximated BLV v_{bl}.

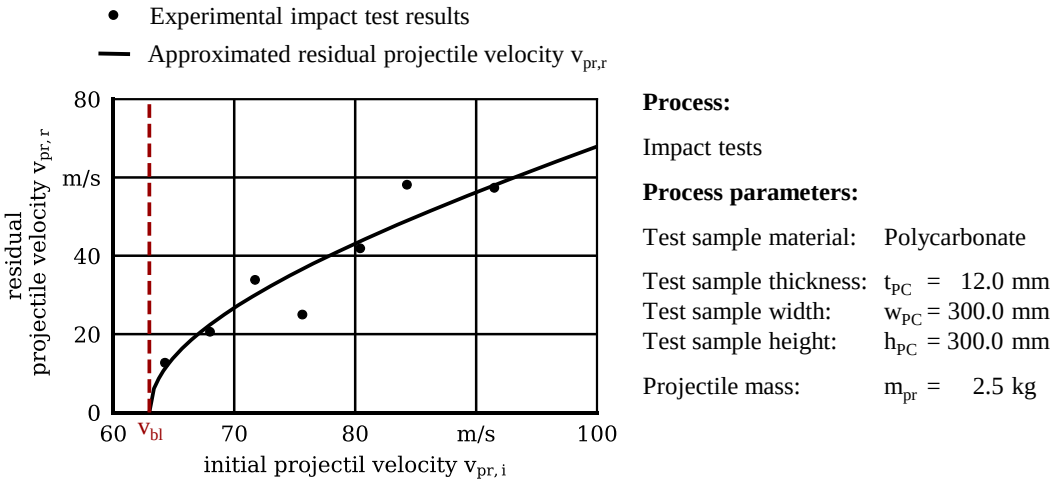

Fig. 4. Exemplary illustration of impact tests results and the approximated BLV v_{bl}

3. SIMULATION MODELL

The FE-simulations were performed using the commercial software LS-DYNA R11.2.2, Ansys, Canonsburg, USA. Figure 5 shows the FE-model in its individual parts used for the simulations. Frame and projectile use a rigid material model that employs the material properties of mild steel with a Young's modulus of $E = 210$ GPa and a density of $\rho = 7.85$ kg/mm^3. The frame consists of shell elements, while the projectile is composed of solid elements. Like the frame, the fastening profiles utilize shell elements and apply a rigid material formulation with the material properties of wood featuring a Young's modulus of $E = 13.4$ GPa and a density of $\rho = 1.2 \cdot 10^{-6}$ kg/mm^3. The PC-sheet is the only part capable of elasto-plastic deformation.

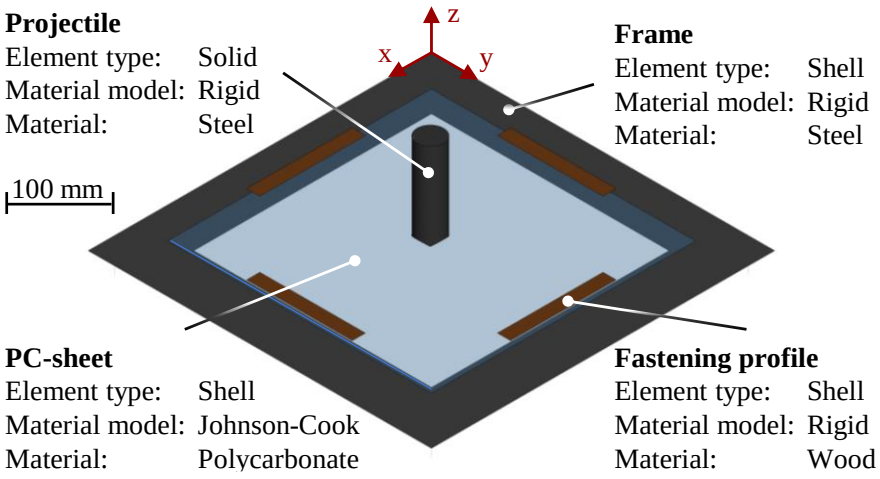

Fig. 5. Parts of the FE-model and the corresponding element and material types

It consists of shell elements, with a finer mesh in the vicinity of the impact point and a coarser mesh towards the frame. A mesh convergence study was conducted with five different sets of element sizes l_E to determine the influence of discretization on the residual projectile velocity $v_{pr,r}$. The parameters of the different meshes as well as their influence on the residual projectile velocity $v_{pr,r}$ are shown in Fig. 6. The maximum residual projectile velocity $v_{pr,r}$ decreases constantly for mesh 1 to mesh 3, as can be seen in Fig. 6b.

a)

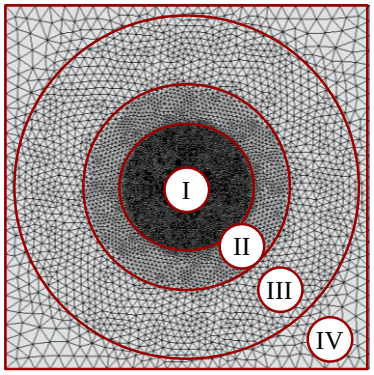

		Average elements size l_E in mm				
		Mesh 1	Mesh 2	Mesh 3	Mesh 4	Mesh 5
Region	I	4.0	3.0	2.0	1.5	1.0
	II	8.0	6.0	4.0	3.0	2.0
	III	16.0	12.0	8.0	6.0	4.0
	IV	32.0	24.0	16.0	12.0	8.0

b)

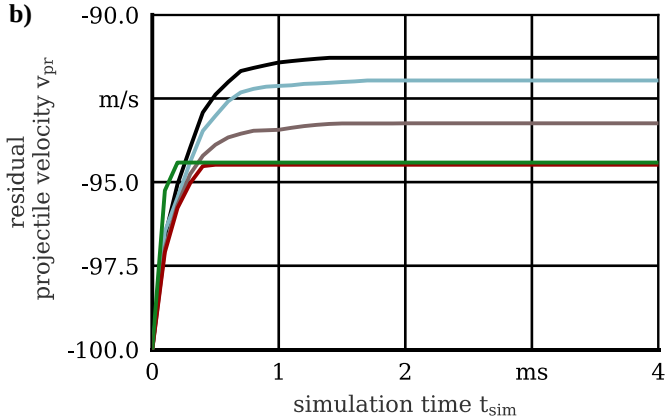

Process:

Impact tests

Process parameters:

Test sample material: Polycarbonate

Test sample thickness: t_{PC} = 12.0 mm
Test sample width: w_{PC} = 300.0 mm
Test sample height: h_{PC} = 300.0 mm

Projectile mass: m_{pr} = 2.5 kg
Initial projectile velocity: $v_{pr,i}$ = 100.0 m/s

Fig. 6. Mesh convergence study: a) Regions of discretization and corresponding mesh parameters; b) Influence of the mesh parameters on the residual projectile velocity v_{pr}

This trend does not continue with mesh 4 and mesh 5, whose results closely match each other. Since a reduction in element size l_E beyond the parameters of mesh 4 only increases the computational cost of the simulation without any significant increase in accuracy, the parameters of mesh 4 are adopted for the further investigation.

The mechanical behavior of PC is characterized by its pronounced dependence on the strain rate $\dot{\varepsilon}$ [16]. To properly describe this behavior of PC a Johnson-Cook (JC) material model was used. Although originally developed for metals, the application has successfully been extended to polymers thus enabling the computation of the plastic response of PC under impact load [17]. In its original form proposed by Johnson and Cook [18] the model incorporates effects such as strain softening, strain hardening as well as thermal softening. However, thermal effects are neglected in the present study since they are considered to have no significant influence mechanical behavior in impact tests. The yield stress σ_y is calculated according to Eq. (2), where A, B, n and C are model parameters, ε_{pl} represents the effective plastic strain, $\dot{\varepsilon}_{pl}$ the strain rate and $\dot{\varepsilon}_0$ a reference strain rate, respectively.

$$\sigma_y = \underbrace{\left(\mathrm{A} + \mathrm{B}\cdot\varepsilon_{pl}^{n}\right)}_{\text{onset of yield and hardening}} \cdot \underbrace{\left(1 + \mathrm{C}\cdot\ln\left(\frac{\dot{\varepsilon}_{\mathrm{pl}}}{\dot{\varepsilon}_0}\right)\right)}_{\text{strain rate } \dot{\varepsilon} \text{ dependence}} \tag{2}$$

The first term in Eq. (2) describes the onset of yield and the hardening, whereas the second term models the yield's dependence on the strain rate $\dot{\varepsilon}$. Failure is introduced into the model via a critical equivalent stress $\sigma_{v,crit}$ and a maximum shear strain γ_{max}, both of which criteria must be satisfied before failure occurs. The JC model parameters are typically of the problem under investigation. Since the tensile testing machine available at the IWF is unable to achieve the high strain rates $\dot{\varepsilon}$ of impact tests, the model parameters of the JC material model were calibrated on the basis of values from Dwivedi et al. [13], who conducted Split Hopkinson Pressure Bar tests at strain rates ranging from $0.005\ \mathrm{s}^{-1} \leq \dot{\varepsilon} \leq 15{,}000\ \mathrm{s}^{-1}$. The experimental data was used to fit the material parameters of the JC-material model. Given that the material constants of Dwivedi et al. [13] are approximated values themselves, they were adopted as the basis for parameter optimization using optimization tool LS-OPT 7.0.0, Ansys, Canonsburg, USA. Contacts were defined between projectile, PC-sheet, frame and fastening profiles. Any displacement or rotation of the frame was constrained by boundary conditions and an initial velocity v_{pr} was applied to the projectile.

4. RESULTS AND DISCUSSION

Figure 7 shows the experimental tensile test results. For the sake of a clear view, only one representative test result per tensile test velocity v_t is presented. The test results of the unaged tensile specimens in Fig. 7a demonstrate the characteristic profile of amorphous thermo-plastics with a strong dependence on the strain rate $\dot{\varepsilon}$, which manifests itself in an increase in yield stress σ_y and a pronounced decrease of the strain at break ε_b towards higher tensile test velocities v_t.

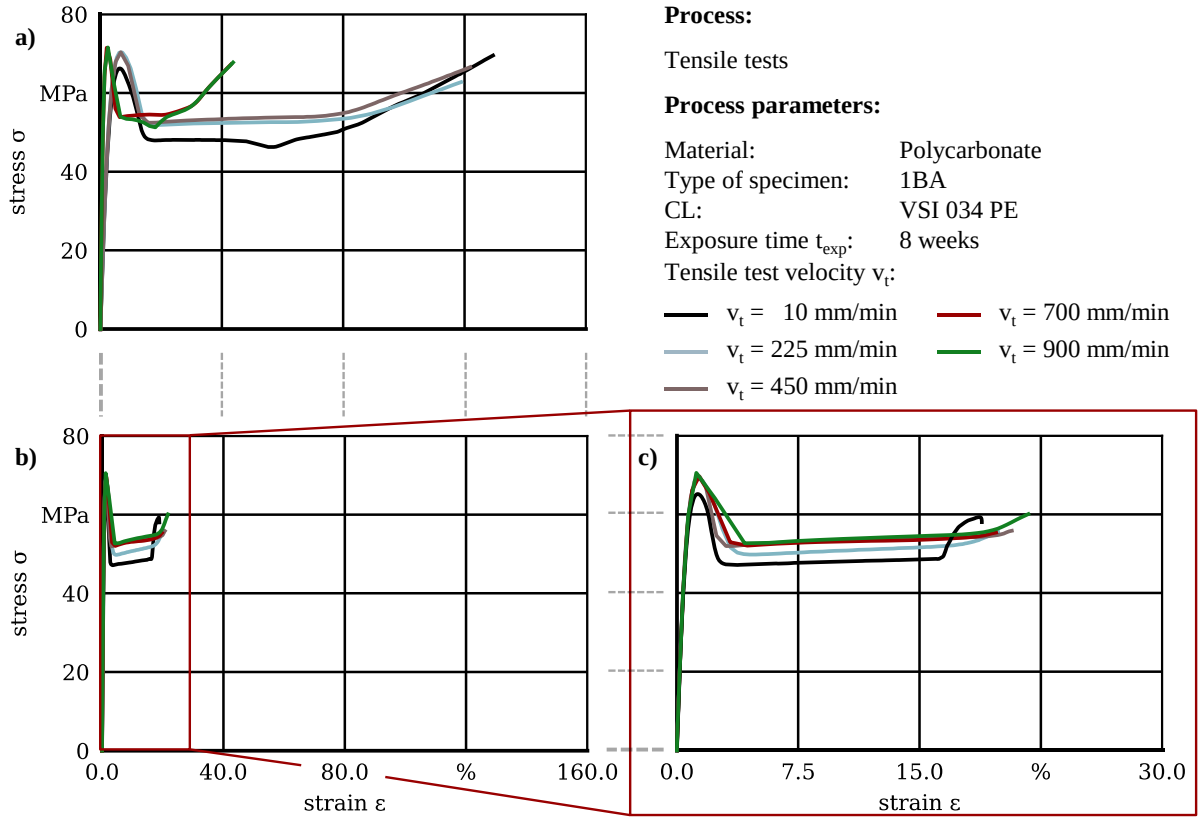

Fig. 7. Tensile test results; a) Test results of the unaged specimen;
b) Test results of the aged specimen; c) Detailed view on the test results of the aged specimen

The test results of the aged specimens depicted in Fig. 7b and 7c, however, suggest that this characteristic behavior is altered by the exposure to CL. The deviation of stress-strain curves of unaged specimen at different strain rates $\dot{\varepsilon}$ is much more pronounced than that of aged specimen, which proceed in a narrow range. Moreover, the strain at break ε_b decreases substantially for all tested strain rates $\dot{\varepsilon}$ when exposed to CL. In contrast, the yield stress σ_y remains virtually unaffected by CL-exposure. Both unaged and aged tensile test results show an almost identical progression and yield stress σ_y level.

The results of the observations in the quasi-static regime translate into a decrease of BVL v_{bl} by 5.7% in the dynamic range, falling from $v_{bl,unaged}$ = 62.9 m/s in the unaged case to $v_{bl,aged}$ = 59.4 m/s after a CL-exposure of t_{exp} = 8 weeks, see Fig. 8. The results of the impact tests and the approximation of the BVL v_{bl} can be found in Table 2 and Table 3 of the appendix. Based on these observations, it is thus concluded, that CL-exposure causes:

- a decrease in BLV v_{bl},
- an earlier onset of failure and
- a vanishing of the dependence on the strain rate $\dot{\varepsilon}$, whereas
- the onset of yield and the hardening remains approximately unaffected.

Using Eq. (2) and the presented influence of parameters *A*, *B*, *n* and *C* of the JC material model, the CL-related decrease of BLV v_{bl} in impact tests is modeled by adopting the aforementioned parameters as well as the failure criteria.

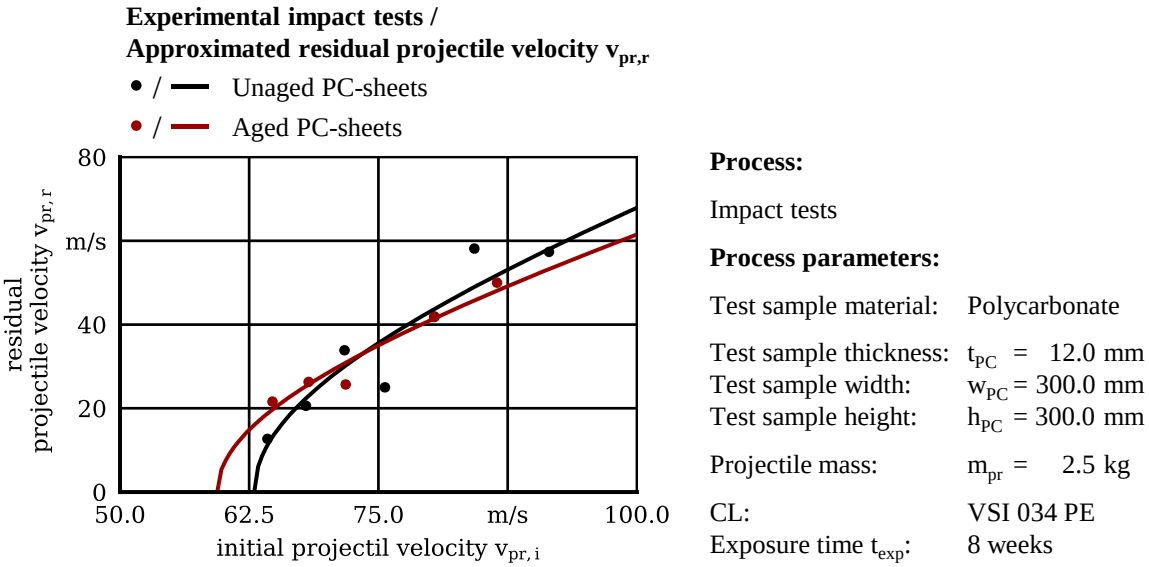

Fig. 8. Experimental impact test results

Since the onset of yield and subsequent hardening are invariant to CL-exposure, the parameters *A*, *B*, and *n* of the unaged and aged model are identical. The vanishing dependence on strain rate $\dot{\varepsilon}$, however, is introduced into the material model by setting the parameter $C \approx 0$ GPa. The reduction of the BLV v_{bl} and the earlier onset of failure is realized by decreasing both failure criteria – the critical equivalent stress $\sigma_{v,crit}$ and the maximum shear strain γ_{max}. Table 1 shows the parameters for both the unaged and aged material model.

Table 1. Material model parameters used for FE-simulations

,	JC model parameters				Failure criterion	
	A in GPa	*B* in GPa	*n*	*C* in GPa	$\sigma_{v,crit}$ in GPa	γ_{max}
Unaged model	0.078	0.066	2.248	0.191	0.335	0.272
Aged model	0.078	0.066	2.248	0.001	0.295	0.249

In Fig. 9 the results of the experimental alongside the FE-simulations are shown. For both – the unaged and the aged material model – the computed BLV v_{bl} is in good agreement with the experiment, showing a maximum deviation of $\Delta v_{bl} = 0.98$ %. Hence, the proposed material model offers an effective way to simulate the ballistic impact on PC-sheets. Furthermore, modeling the decrease of BVL v_{bl} by adjusting the JC material parameters and failure criteria has been demonstrated to accurately represent CL-related aging. It is also evident, however, that the agreement between experiment and simulation is best for low projectile velocities $v_{pr,i}$ close to the BLV v_{bl}. The deviation between experimental and simulated results tends to increase with increasing projectile velocity $v_{pr,i}$, which suggests that the proposed material model does not capture all relevant physical effects involved in impact.

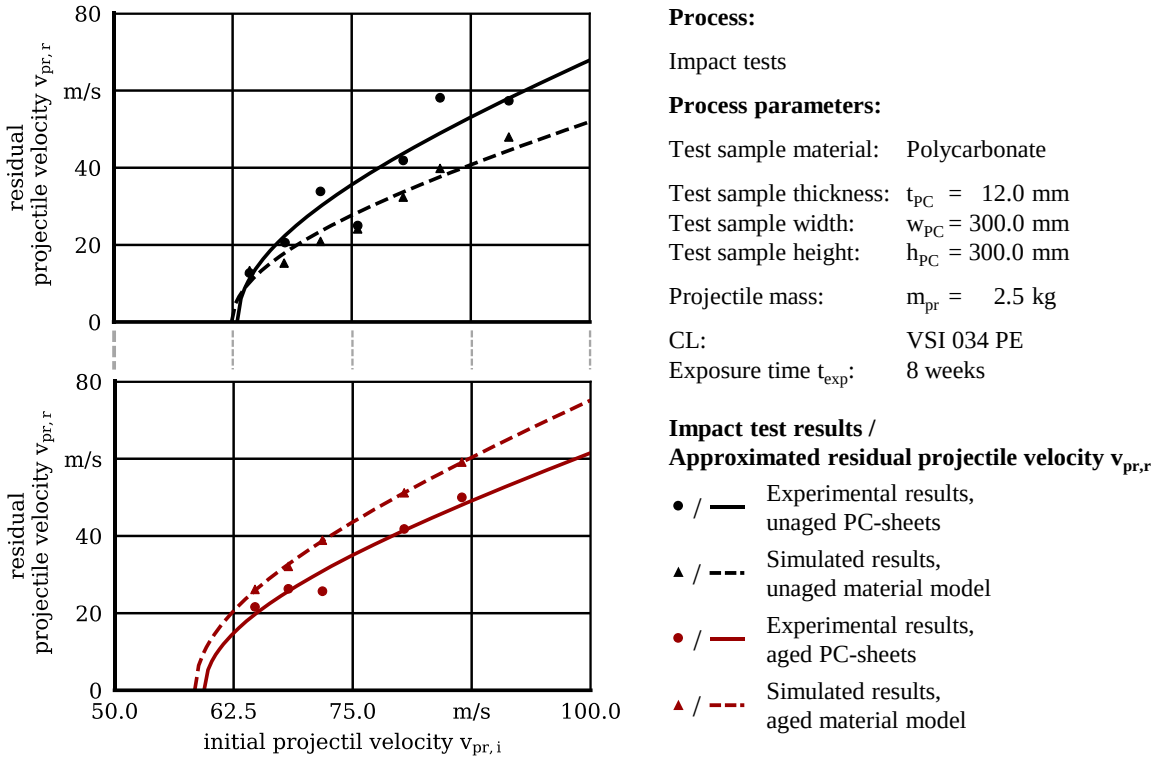

Fig. 9. Comparison of experimental and simulated impact test results

5. CONCLUSION

In the present work, a method for modeling CL-related aging of PC-sheets under impact loading was presented. For this purpose, PC-specimen and -sheets were exposed to an CL-emulsion in immersion bath tests for a total exposure time of t_{exp} = 8 weeks. Besides a decrease in BLV v_{bl}, the experiments indicate that CL-related aging affects the material's dependence on the strain rate $\dot{\varepsilon}$, whereas the onset of yielding and the subsequent strain hardening are invariant to aging. These observations were incorporated into a simulation model utilizing a JC material model. Aging was introduced via an adaptation of the parameter C of the JC material model and the failure criteria. The model is capable to determine the BLV v_{bl} with a maximum deviation of Δv_{bl} = 0.98 %. However, an increasing deviation between experiment and simulation towards higher projectile velocities $v_{pr,i}$, indicates, that not all relevant physical effects involved in impact are captured by the model. Future work will be dedicated to a more in-depth analysis of the mechanisms involved in aging with the goal to increase the accuracy of the FE-model. Nevertheless, the presented simulation model demonstrates that the CL-related decrease in BLV v_{bl} can be computed with high accuracy.

ACKNOWLEDGEMENTS

The authors would like to thank BSA Kunststofftechnik GmbH, Gütersloh, Germany for providing the material used for the experimental investigation.

REFERENCES

[1] NEUDÖRFER A., 2021, *Konstruieren Sicherheitsgerechter Produkte*, Springer Berlin Heidelberg, Berlin, Heidelberg.
[2] DIN EN ISO, 14120, 2015 *Safety of Machinery – Guards - General Requirements for Design and Construction of Fixed and Movable Guards*, ISO Copyright Office, Vernier, Geneva.
[3] DIN EN ISO, 23125, 2015, *Machine Tools – Safety – Turning Machines*, ISO Copyright Office, Vernier, Geneva.
[4] BEN-DOR G., DUBINSKY A., ELPERIN T., 2013, *High-Speed Penetration Dynamics*, World Scientific Publishing, Singapore.
[5] LANDI L., UHLMANN E., HÖRL R., THOM S., GIGLIOTTI G., STECCONI A., 2022, *Evaluation of Testing Uncertainties for the Impact Resistance of Machine Guards*, ASCE-ASME J. Risk and Uncert., Engrg. Sys., Part B, Mech. Engrg., 2.
[6] UHLMANN E., POLTE M., HÖRL R., BERGSTRÖM N., THOM S., WITTWER P., 2021, *Experimental Investigation of the Kink Effect by Impact Tests on Polycarbonate Sheets*, Proceedings of the 31st European Safety and Reliability Conference.
[7] LANDI L., PERA F., MORETTINI G., DEL PRETE E., RATTI C., 2022, *Ejection Test Requirements for Parts of Machine Tools: Part 2 Testing Energy Equivalence Hypothesis and Weak Points of Vision Panels,* Proceedings of the 32nd European Safety and Reliability Conference (ESREL 2022).
[8] BOLD J., 2004, *Trennende Schutzeinrichtungen für Werkzeugmaschinen zur Hochgeschwindigkeitsbearbeitung,* Dissertation, Technische Universität Berlin.
[9] DUCHSTEIN B., 2010, *Aufprallprüfungen an Definiert Gealterten Polycarbonat Sichtscheiben,* Futur: Vision, Innovation, Realisierung, Mitteilungen aus dem Produktionstechnischen Zentrum (PTZ), 1, 6–7.
[10] LAU K., 2006, *Plasmagestützte Aufdampfprozesse für die Herstellung Haftfester Optischer Beschichtungen auf Bisphenol-A Polycarbonat*, Dissertation, Martin-Luther-Universität Halle-Wittenberg.
[11] LANDI L., STECCONI A., VITTORI M., PERA F., 2021, *Effect of Sunlight Exposition on Withstanding Capability of Thin Polycarbonate Sheets*, Proceedings of the 31st European Safety and Reliability Conference.
[12] UHLMANN E., HABERBOSCH K., THOM S., DRIEUX S., SCHWARZE A., POLTE M., 2019, *Investigation on the Effect of Novel Cutting Fluids with Modified Ingredients Regarding the Long-Term Resistance of Polycarbonate Used as Machine Guards in Cutting Operations (KSS-PC)*, Proceedings of the 29th European Safety and Reliability Conference.
[13] DIN EN ISO, 527–2, 2012, *Plastics - Determination of Tensile Properties*, ISO Copyright Office, Geneva.
[14] DWIVEDI A., BRADLEY J., CASEM D., 2012, *Mechanical Response of Polycarbonate with Strength Model Fits*, Aberdeen.
[15] RECHT R.F., IPSON T.W., 1963, *Ballistic Perforation Dynamics*, Journal of Applied Mechanics, 30, 384–390.
[16] LAMBERT J.P., JONAS G.H., 1976, *Towards Standarization in Terminal Ballistic Testing: Velocity Representation*, Maryland.
[17] SARVA S., MULLIKEN A.D., BOYCE M.C., 2007, *Mechanics of Taylor Impact Testing of Polycarbonate*, International Journal of Solids and Structures, 7–8, 2381–2400.
[18] STOMMEL M., 2011, *FEM zur Berechnung von Kunststoff- und Elastomerbauteilen*, Hanser Verlag, München.
[19] JOHNSON G.R., COOK W.H., 1983, *A Constitutive Model and Data for Metals Subjected to Large Strains, High Strain Rates and High Temperatures*, Proceedings 7th International Symposium on Ballistics, 21, 541–547.

APPENDIX

Table 2. Impact test results

	Experimental impact test results		Simulated impact test results	
	Initial projectile velocity $v_{pr,I}$ in m/s	Residual projectile velocity $v_{pr,r}$ in m/s	Initial projectile velocity $v_{pr,I}$ in m/s	Residual projectile velocity $v_{pr,r}$ in m/s
Unaged PC-sheets	64.3	12.7	64.3	13.4
	67.9	20.6	67.9	15.3
	71.7	33.9	71.7	20.9
	75.6	25.0	75.6	24.2
	80.4	41.9	80.4	32.4
	84.3	58.1	84.3	39.8
	91.5	57.4	91.5	48.0
Aged PC-sheets	64.8	21.6	64.8	26,2
	68.3	26.3	68.3	32.1
	71.8	25.7	71.8	38.9
	80.4	41.8	80.4	51.2
	86.5	50.0	86.5	59.1

Table 3. Parameters of analytical model by Recht and Ipson [15]

	Experimental results		Simulated results	
	Parameter a	BLV v_{bl} in m/s	Parameter a	BLV v_{bl} in m/s
Unaged PC-sheets	0.9	63.0	0.7	62.0
Aged PC-sheets	0.8	59.4	0.9	58.4